QCD STUDIES AND α_S MEASUREMENTS AT LEP

STEFAN SÖLDNER-REMBOLD
University of Manchester, Oxford Road, M13 9PL, Manchester, UK
E-mail: soldner@fnal.gov

The LEP experiments have measured event shapes using data taken at e^+e^- center-of-mass energies $\sqrt{s}$ ranging from 91 GeV to 209 GeV. Using the final LEP event shape measurements, a combined value of the strong coupling constant $\alpha_s(M_Z)$ has been extracted. Events with photon radiation have been used to extend the measurements to lower center-of-mass energies $\sqrt{s'}$ to study the running of α_s. Alternative α_s measurements using four-jet rates have also been performed.

1 Data Sample

Between 1989 and 2000 the four LEP experiments have taken data at e^+e^- center-of-mass energies $\sqrt{s}$ ranging from 91 GeV to 209 GeV. Each experiment has collected several million multi-hadronic events at $\sqrt{s} = M_Z$. At higher energies about 10^3 events have been recorded per energy point. After a basic event selection, no significant background remains at $\sqrt{s} = M_Z$. In the range $\sqrt{s} > 2M_W$ the background rate is about $10-15\%$ due to four-fermion production in $e^+e^- \to W^+W^-$ events. For an accurate determination of $\sqrt{s}$ it is also important to identify and reconstruct events with initial and final state photon radiation.

2 Event Shape Observables

The properties of hadronic events may be described by a set of event shape observables. These may be used to characterize the distribution of particles in an event as "pencil-like", planar, spherical, etc. They can be computed either using the measured charged particles and calorimeter clusters, or using the hadrons or partons in simulated events. In order that predictions of perturbative QCD be reliable, it is necessary that the value of the observable be infra-red stable (i.e. unaltered under the emission of soft gluons) and collinear stable (i.e. unaltered under collinear parton branchings). The following event shapes are considered here:

Thrust T: defined by the expression

$$T = \max_{\vec{n}} \left(\frac{\sum_i |p_i \cdot \vec{n}|}{\sum_i |p_i|} \right),$$

where p_i is the three-momentum of particle i. The thrust axis $\vec{n}_T$ is the direction $\vec{n}$ which maximizes the expression in parentheses. A plane through the origin and perpendicular to $\vec{n}_T$ divides the event into two hemispheres.

***C*-parameter:** The linearized momentum tensor is given by

$$\Theta^{\alpha\beta} = \frac{\sum_i (p_i^\alpha p_i^\beta)/|p_i|}{\sum_i |p_i|} \quad (\alpha, \beta = 1, 2, 3),$$

where the sum runs over particles, i, and α, β denote the Cartesian coordinates of the momentum vector. The three eigenvalues λ_j of this tensor define C through

$$C = 3(\lambda_1\lambda_2 + \lambda_2\lambda_3 + \lambda_3\lambda_1).$$

Heavy Jet Mass M_H: The hemisphere invariant masses are calculated using the particles in the two hemispheres. M_H is the heavier of the two masses.

Jet Broadening B_T and B_W: These are defined by computing the quantity

$$B_k = \left(\frac{\sum_{i \in H_k} |p_i \times \vec{n}_T|}{2 \sum_i |p_i|} \right)$$

for each of the two hemispheres. The two observables are defined by

$$B_T = B_1 + B_2 \quad \text{and} \quad B_W = \max(B_1, B_2),$$

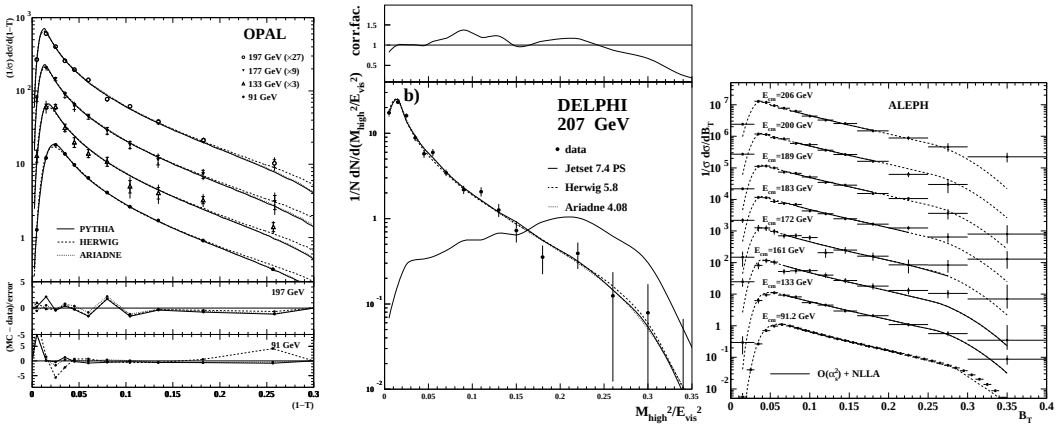

Figure 1. (left) $1-T$ measured by OPAL in the range $\sqrt{s} = 91-197$ GeV. (center) M_H measured by DELPHI at $\sqrt{s} = 207$ GeV. The subtracted four-fermion background is shown separately. The OPAL and DELPHI data are compared to PYTHIA (JETSET), HERWIG and ARIADNE MC simulations. (right) B_T measured by ALEPH in the range $\sqrt{s} = 91 - 206$ GeV. The continuous line shows the region where the $\mathcal{O}(\alpha_s^2)$+NLLA fit has been performed.

where B_T is the total and B_W is the wide jet broadening.

Transition between 2- and 3-jets (y_{23}): The value of the jet resolution parameter, $y_{\rm cut}$, at which the event makes a transition between a 2-jet and a 3-jet assignment, for the Durham jet finding scheme [1].

The final results on event shapes have recently been published by all four LEP collaborations [2,3,4,5]. Examples are shown in Fig. 1. The agreement between data and Monte Carlo (MC) simulations is in general very good which justifies the use of simple bin-by-bin efficiency corrections.

The QCD calculations for the cumulative cross-section $R(y) \equiv \int_0^y \frac{1}{\sigma}\frac{{\rm d}\sigma}{{\rm d}y}{\rm d}y$ as a function of the event shape variable $y(y = 1-T, C, M_H, B_T, B_W, y_{23})$ can be performed in the next-to-leading-logarithmic approximation (NLLA) or using a fixed order $\mathcal{O}(\alpha_s^2)$ calculation. The $\mathcal{O}(\alpha_s^2)$ prediction is expected to be best for the multi-jet region (high y), whereas the NLLA prediction is best for the two-jet region (low y). The "log(R)" matching scheme is adopted for combining the $\mathcal{O}(\alpha_s^2)$ and NLLA predictions. In the log(R) matching scheme the terms up to $\mathcal{O}(\alpha_s^2)$ in the NLLA expression are replaced by the $\mathcal{O}(\alpha_s^2)$ terms from $\log R_{\mathcal{O}(\alpha_s^2)}$.

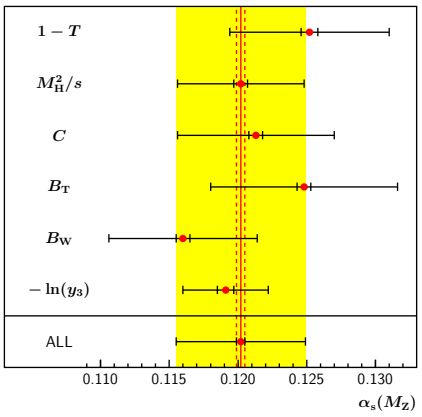

Figure 2. Combined $\alpha_s(M_Z)$ for the six event shape variables measured by the four LEP experiments. The inner error bar is the statistical, the outer error bar is the total uncertainty [6].

Each experiment has performed α_s fits using these predictions for the six event shape variables at different $\sqrt{s}$. A preliminary combination of these results, taking into account the correlations between the sources of un-

certainties, yields [6]

$$\alpha_s(M_Z) = 0.1202 \pm 0.0003(\text{stat}) \pm 0.0007(\text{expt}) \pm 0.0015(\text{hadr}) \pm 0.0044(\text{theo})$$

with $\chi^2/\text{d.o.f.} = 93/166$. The combined α_s measurements for each event shape variable are shown in Fig. 2 and the combined α_s measurements for each experiment in Fig. 3.

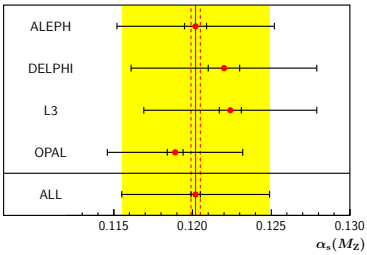

Figure 3. Combined $\alpha_s(M_Z)$ for the four LEP experiments using the measurements from the six event shape variables. The inner error bar is the statistical, the outer error bar is the total uncertainty [6].

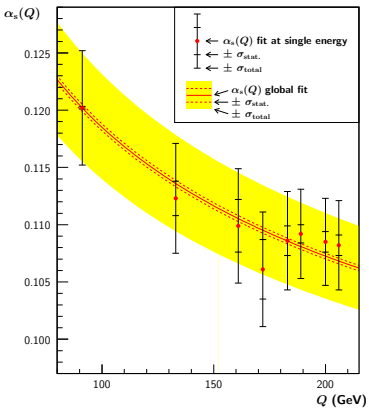

Figure 4. The running of α_s as a function of $Q = \sqrt{s}$ using the combined LEP data. The inner error bar is the statistical uncertainty, the outer error bar is the total uncertainty [6].

The experimental uncertainty includes uncertainties from cut variation, detector corrections and background subtraction. The hadronization uncertainty is determined by performing the hadronization correction using different MC generators (HERWIG, ARIADNE, PYTHIA. The theoretical uncertainty includes the variation of the renormalization scale, $0.5 < x_\mu < 2$, the variation of the logarithmic rescaling factor, $2/3 < x_L < 3/2$, and of kinematic cut-off parameters. In addition, the $\log(R)$ matching scheme is replaced by the R matching scheme [7].

The running of α_s using the combined data is shown in Fig.4. Although the statistical precision of the LEP1 data at $\sqrt{s} = M_Z$) is much higher, the LEP1 and LEP2 data have about equal weight in the combined fit because of the smaller hadronization and theory uncertainties at larger $\sqrt{s}$.

3 α_s from Radiative Events

Radiative hadronic events have been used to extend the range of center-of-mass energies below $\sqrt{s} = M_Z$. Assuming that initial state or final state photons do not interfere with the QCD process [8], a measurement of α_s at a reduced center-of-mass energy $\sqrt{s'}$ is possible by identifying isolated high energy photons in the detector [9].

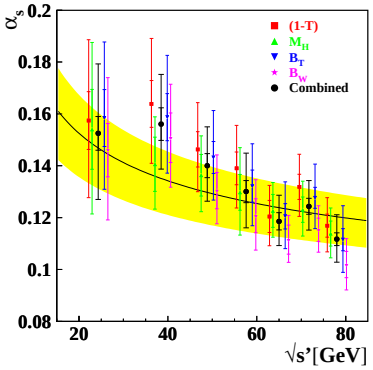

Figure 5. The running of α_s as a function of $Q = \sqrt{s'}$ using radiative hadronic events measured by OPAL [10]. The result of the α_s fit is shown as continuous line.

In the analysis performed by OPAL [10] photons have been separated from the dominant π^0 background by using a likelihood based on cluster shape fits in the calorimeter. The running of α_s as function of $\sqrt{s'}$ is

Table 1. Summary of the $\alpha_s(M_Z)$ results presented in this talk.

	data	theory	$\alpha_s(M_Z)$	stat	expt	hadr	theo
LEP	event shapes	$\mathcal{O}(\alpha_s^2)$+NLLA	0.1202	0.0003	0.0007	0.0015	0.0044
OPAL	radiative events	$\mathcal{O}(\alpha_s^2)$+NLLA	0.1176	0.0012		$^{+0.0093}_{-0.0085}$	
OPAL	R_4/Durham	$\mathcal{O}(\alpha_s^3)$+NLLA	0.1208	0.0006	0.0021	0.0019	0.0024
DELPHI	R_4/Cambridge	$\mathcal{O}(\alpha_s^3)$+$x_\mu^{\rm opt}$	0.1175	0.0005	0.0010	0.0027	0.0007

shown in Fig. 5. The result of the α_s fit is given in Table 1.

4 Power Law Corrections

Non-perturbative effects in event shape observables are usually suppressed by powers of $1/Q$ [11]. The corresponding hadronization corrections at LEP energies are of the order 10%. These hadronization corrections can be determined using MC generators or by analytical power law calculations. These calculations introduce one additional phenomenological parameter α_0,

$$\alpha_0(\mu_I) = \frac{1}{\mu_I}\int_0^{\mu_I} \alpha_s(k)\mathrm{d}k,$$

which measures the effective strength of the strong coupling up to an infrared matching scale of $\mu_I \approx 1$ GeV. The parameter α_0 is expected to be universal and must be determined by experiment.

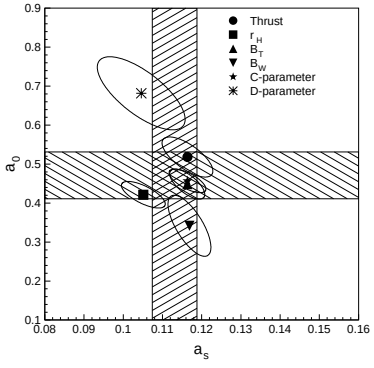

Figure 6. Contours of confidence levels for simultaneous measurements of α_s and α_0 measured by L3 using the first moments of event shape variable. The unweighted averages are shown as shaded bands. A 4-jet observable (D parameter) is also shown.

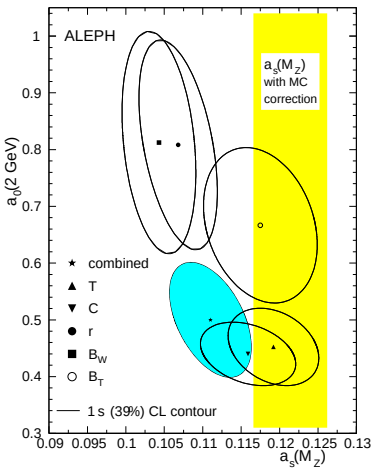

Figure 7. Contours of confidence levels for simultaneous measurements of α_s and α_0 compared to the α_s measurement using MC corrections (shaded band).

The result of such a combined fit, performed by L3 [4] for the first moments of the event shape variables, is shown in Fig. 6. The six values of α_0 obtained from the event-shape variables do not agree well. A similar result has been obtained by DELPHI [3]. A large spread of α_0 values has also been observed by ALEPH [2] using event shape distributions. The resulting α_s is significantly lower than the result obtained using MC hadronization corrections (Fig. 7).

5 α_s from Four-jet Rates

An alternative method to determine α_s is to measure four-jet rates, since the jet rates are predicted as functions of the jet resolution parameter with α_s as free parameter. OPAL [12] has measured the four-jet rates using the Durham jet finding algorithm [1] as

a function of the jet resolution parameter (Fig. 8). The strong coupling α_s is fitted using a $\mathcal{O}(\alpha_s^3)$+NLLA matched calculation of the four-jet rates.

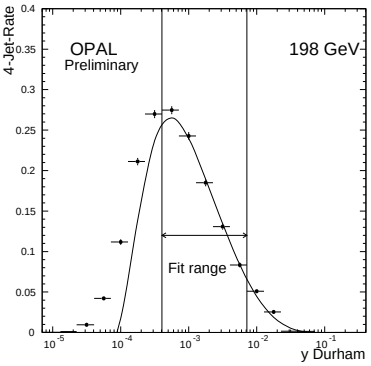

Figure 8. A fit to the four-jet rate R_4 measured at $\sqrt{s} = 198$ GeV.

In a similar analysis, DELPHI [13] has measured the four-jet rates using the Durham and the Cambridge [14] algorithms. The data are fitted using a fixed order $\mathcal{O}(\alpha_s^3)$ calculation with both α_s and the renormalization scale x_μ as free parameter. To determine the experimentally optimized scale, a two parameter fit with α_s and $x_\mu^{\rm opt}$ as free parameters has also been performed (Fig. 9). Due to a smaller theoretical uncertainty the α_s fit using the Cambridge algorithm is quoted as final result (Table 1).

6 Summary

A preliminary α_s combination using the final event shape measurements of all four LEP experiments has been presented. The universality of power law corrections has been studied. Radiative events and four-jet events have been used to study the running of α_s.

Acknowledgments

Special thanks to Matthew Ford for performing the α_s combination and to Roger Jones, Stefan Kluth, Gavin Salam and Daniel Wicke for their help in preparing this presentation.

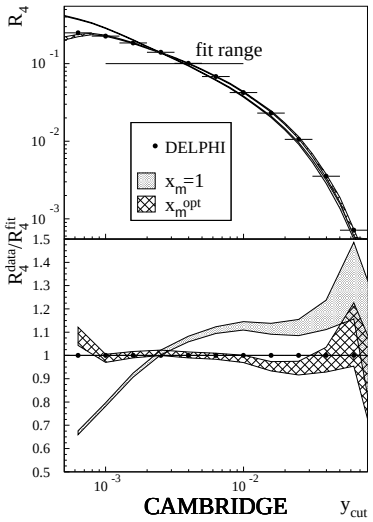

Figure 9. Fits to the four-jet rates R_4 measured at $\sqrt{s} = M_Z$ using the Cambridge algorithm. The grey band shows a fit with the physical scale ($x_\mu = 1$) and the cross-hatched band a fit with optimized scales.

References

1. S. Catani et al., *Phys. Lett.* B **269**, 432 (1991).
2. ALEPH Coll., A. Heister et al., *Eur. Phys. J.* C **35**, 457 (2004).
3. DELPHI Coll., J. Abdallah et al., *Eur. Phys. J.* C **37**, 1 (2004).
4. L3 Coll., P. Achard et al., *Phys. Rept.* **399**, 71 (2004).
5. OPAL Coll., G. Abbiendi et al., CERN-PH-EP/2004-044, subm. to EPJC.
6. M. Ford and the LEP QCD Working Group, private communications.
7. R.W.L. Jones et al., *JHEP* **12**, 7 (2003).
8. M. Dasgupta, G.P. Salam, *J. Phys.* G **30** R143 (2004), footnote 6.
9. L3 Coll., M. Acciarri et al., *Phys. Lett.* B **411**, 339 (1997)
10. OPAL Coll., PN519 and abstract 5-0515.
11. Y. Dokshitzer, B.R. Webber, *Phys. Lett.* B **404**, 321 (1997) and ref. therein.
12. OPAL Coll., PN527 and abstract 5-0600.
13. DELPHI Coll., J. Abdallah et al., hep-ex/0410071, subm. to EPJC.
14. Y. Dokshitzer et al., *JHEP* **8**, 1 (1997).